DEUTSCHES ELEKTRONEN-SYNCHROTRON DESY

DESY SR-83-07
June 1983

F-BONDING IN PRASEODYMIUM METAL UNDER HIGH PRESSURE

by

W.A. Großhans and W.B. Holzapfel

Universität - GH - Paderborn, Federal Republic of Germany

Y.K. Vohra

Bhabha Atomic Research Centre, Trombay, Bombay - 400085, INDIA

ISSN 0723-7979

NOTKESTRASSE 85 · 2 HAMBURG 52

To be sure that your preprints are promptly included in the
HIGH ENERGY PHYSICS INDEX ,
send them to the following address (if possible by air mail) :

DESY
Bibliothek
Notkestrasse 85
2 Hamburg 52
Germany

DESY SR-83-07
June 1983

ISSN 0723-7979

F-BONDING IN PRASEODYMIUM METAL UNDER HIGH PRESSURE

W. A. Großhans[a], Y. K. Vohra[b] and W. B. Holzapfel[a]

(a) Experimentalphysik, Universität - GH - Paderborn, D-4790 Paderborn, Federal Republic of Germany

(b) Neutron Physics Division, Bhabha Atomic Research Centre, Trombay, Bombay - 400085, INDIA

ISCU/AB-6110, 6155F

ABSTRACT

High pressure X-ray diffraction studies up to 40 GPa on Praseodymium (Pr) metal reveal the presence of α-Uranium structure above 20 GPa. The appearance of this structure is related to the participation of f electrons in bonding, in close analogy with Cerium (Ce) and Americium (Am).

"Journal of Physics F: Metal Physics" in press

It is now generally accepted that the 4f electrons are localized at ambient conditions in all the lanthanides (Lanthanum to Lutetium) and, therefore, do not contribute to bonding (Johannsson and Rosengren 1975, Johannsson et al. 1981). Only the three spd electrons in the conduction band and the sp → d electron transfer under pressure determine the crystal structures at ambient conditions as well as the high pressure phase transitions in the regular lanthanides (Duthie and Pettifor 1977, Vohra et al. 1981).

The special properties of the light lanthanide Cerium (Ce) at low temperatures and at high pressures, however, are generally attributed to 4f electron delocalization (Johannsson 1974) and, similarly, the light actinides show special features due to itinerant 5f electrons, e.g. high cohesive energies, low melting points and low symmetry crystal structures, whereas the heavy actinides, from Am on, show close similarity to the lanthanides and are considered to have only localized 5f electrons. Furthermore, it is generally recognized that application of pressure on light rare earths (Ce, Pr, ...) and heavy actinides (Am, Cm, ...) can force the localized f^n configuration to participate in bonding. A Mott transition picture has been suggested for a localization ⇌ delocalization transition in lanthanide and actinide elements (Johannsson 1974). Also, experimentally, a typical light actinide crystal structure (α-Uranium) has been identified in Ce between 5 GPa to 13 GPa (Zachariasen and Ellinger 1975) and in Am above 15 GPa (Roof et al. 1980). 4f-delocalization was reported also for Pr under pressure (Mao et al. 1981), where a new phase above 20 GPa was indexed as hexagonal with a related volume collapse of 19 %. This study stimulated our present work since the volume collapse appeared to be unusually large and related to an ambiguous indexing of the diffraction patterns.

In the present study, the Pr metal was studied up to 40 GPa by energy dispersive X-ray diffraction in a diamond anvil cell (Holzapfel and May 1982). The ruby R_1 fluorescence method has been used for pressure measure-

ment (Piermarini et al. 1975). Pr metal crystallizes in double hexagonal close packed structure (dhcp) at ambient conditions. In the pressure range 0 - 20 GPa, similar to the previous investigation (Mao et al. 1981), the regular sequence of rare earth phase transitions was observed: dhcp $\xrightarrow{4\ GPa}$ fcc $\xrightarrow{6.2\ GPa}$ distorted fcc. This sequence results from s → d transfer within the trivalent metallic configuration, with no bonding contribution from f electrons (Großhans et al. 1982).

Between 18 GPa and 21 GPa, a sluggish transition to the collapsed phase was noticed. Fig. 1 shows the energy dispersive X-ray diffraction (EDX) pattern of Pr at a pressure of 26.2 GPa in this phase, where the indexing of the diffraction lines is given with respect to an orthorhombic cell (α-Uranium, D_{2h}^{17} - Cmcm) with 4 atoms per cell, giving an atomic volume of V = 18.88 Å^3. The same indexing can be used for the diffraction pattern of Pr at 23.3 GPa given by Mao et al. (1981). Table 1 compares the α-Uranium indexing with the hexagonal indexing proposed by Mao et al. (1981), using their original data set. It can be seen that α-Uranium structure fits the observed d_{hkl} values also within their experimental accuracy, especially if one considers the typical effects of nonhydrostatic stress (Singh and Kennedy 1974, Syassen and Holzapfel 1978). The α-Uranium indexing of these data gives a = 2.761 Å, b = 5.618 Å, c = 4.877 Å, V = 18.91 Å^3/atom, which is very close to our value at 26.2 GPa. This results in a volume collapse of 9.3 % at 21 GPa in contrast to the 19 % collapse required by the hexagonal indexing of Mao et al. (1981). Since the atom positions in the hexagonal unit cell were not specified by Mao et al. (1981), the intensity data can be compared only with theoretical values for the α-Uranium structure, and even in this case the comparison can be only qualitative, since effects of texture and various absorption corrections are ambiguous. Table 1 shows, that the dominant features of the experimental intensity ratios are well reproduced by the theoretical ratios for the α-Uranium structure and the present intensity ratios indicate the same trend, taking into account that the EDX-data have to be evaluated with different corrections on the primary intensity.

Both, the intensity ratios and the smaller volume callapse support the α-Uranium indexing.

Finally, it should be noted that the occurence of the α-Uranium structure in Pr metal under pressure nicely fits into the systematics of crystal structures of lanthanides and actinides, where this structure appears under pressure if a critical amount of f-character is admixed to the valence band. High pressure experiments on Ce and Am, and now also on Pr support this point of view.

One of us (Y.K.V.) is grateful to Alexander von Humboldt-Foundation for grant of a fellowship.

Part of this work was performed at HASYLAB and has been supported by the Bundesministerium für Forschung und Technologie.

REFERENCES

Duthie , J. C. and Pettifor D. G., 1977, Phys. Rev. Lett. 38, 564

Großhans, W. A., Vohra, Y. K. and Holzapfel, W. B., 1982, Phys. Rev. Lett. 49, 1572

Holzapfel, W. B. and May, W., 1982, in Advances in Earth and Planetary Sciences, Vol. 12; High Pressure Research in Geophysics, eds. S. Akimoto and M. H. Manghnani, 73

Johannsson, B., 1974, Phil. Mag. 30, 469

Johannsson, B. and Rosengren, A., 1975, Phys. Rev. B11, 2836

Johannsson, B., Skriver, H. L. and Andersen, O. K., 1981, in Physics Of Solids Under High Pressure, eds. J. S. Schilling and R. N. Shelton (North Holland, Amsterdam), 245

Mao, H. K., Hazen, R. M., Bell, P. M. and Wittig, J., 1981, J. Appl. Phys. 52, 4572

Piermarini, G. J., Block, S., Barnett, J. D. and Forman, R. A., 1975, J. Appl. Phys. 46, 2774

Roof, R. B., Haire, R. G., Schiferl, D., Schwalbe, L. A., Kmetko, E. A. and Smith, J. L., 1980, Science 207, 1353

Singh, A. K. and Kennedy, G. C., 1974, J. Appl. Phys. 45, 4686

Syassen, K. and Holzapfel, W. B., 1978, Rev. Sci. Instr.49, 1107

Vohra, Y. K., Olijnyk, H., Großhans, W. A. and Holzapfel, W. B., 1981, Phys. Rev. Lett. 47, 1065

Zachariasen, W. H. and Ellinger, F. H., 1975, Acta Cryst. A33, 155

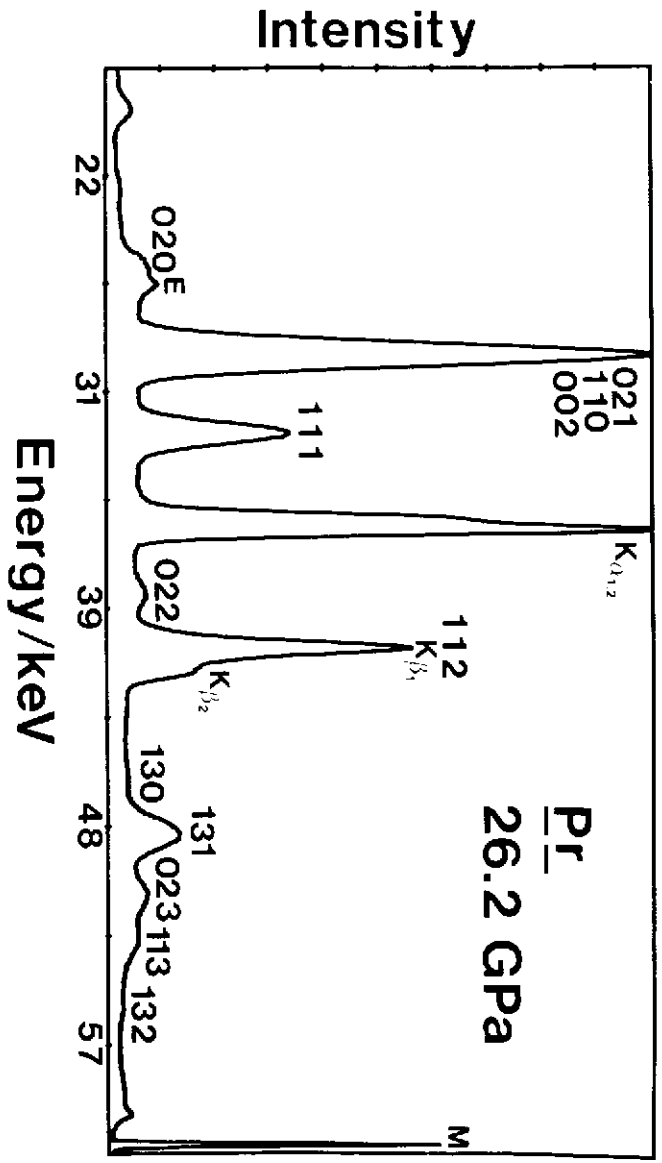

Fig. 1 EDX pattern for Pr at a pressure of 26.2 GPa with α-Uranium indexing using a = 2.757 Å, b = 5.604 Å and c = 4.889 Å. Indices of very weak lines are omitted.
E: escape peak, M: marker.

Table 1 Comparison of hexagonal and α-Uranium indexing for the data given by Mao et al. (1981) for Pr at 23.3 GPa. The calculated intensities are for space group Cmcm, Pr at position 4(c) with y = 0.1.

$d_{obs}/\mathring{A}$	$d_{hex}/\mathring{A}$	$d_{\alpha - U}/\mathring{A}$	hkl	(I/I_o) / % calc	obs
2.816	2.816	2.809	020	8	40
2.482	2.481	2.478	110	76	50
2.431	2.438	2.438 2.434	002 021	56 100	100
2.209	2.211	2.209	111	57	80
1.842	1.843	1.842	022	4	10
1.738	1.738	1.738	112	48	70
1.550	1.545	1.550	130	2	5
1.477	1.480	1.477	131	36	80
1.406	1.408	1.407	023	15	40
-	-	1.381	200	7	0
1.354	1.354	1.359	113	10	30
1.305	1.305	1.308	132	2	5
1.203	1.202	1.201	221	17	50